Linearly polarized Cu *K*-edge absorption spectroscopy of $CuGeO_3$: Orbital population, band dispersion, and exchange interactions

D. Z. Cruz, M. Abbate,* and H. Tolentino
Laboratório Nacional de Luz Síncrotron, Caixa Postal 6192, 13083-970 Campinas SP, Brazil

P. J. Schiling and E. Morikawa
Center for Advanced Microstructures and Devices, Louisiana State University, 3990 West Lakeshore Drive, Baton Rouge, Louisiana 70803

A. Fujimori
Department of Physics, University of Tokyo, Bunkyo-ku, Tokyo 113, Japan

J. Akimitsu
Department of Physics, Aoyama Gakuin University, Chitosedai, Setagaya-ku, Tokyo 157, Japan

(Received 25 August 1998)

We studied the unoccupied electronic states of $CuGeO_3$ using linearly polarized Cu *K*-edge absorption spectroscopy. The spectra show structures related to the Cu $4p_z$ band with $\mathbf{E}\|c$ axis and to the Cu $4p_y$ band with $\mathbf{E}\|b$ axis. The Cu $4p_z$ band appears at higher energies than the Cu $4p_y$ band due to the stronger interactions with the O $2p$ levels. The Cu $4p$ spectral weight is split about 5 eV into the so-called *well screened* and *poorly screened* peaks. The Cu $4p$ bands exhibit changes as a function of the angle θ between the polarization vector and the *c* axis. The intensity changes reflect the polarization and the energy shifts reflect the dispersion of the Cu $4p$ bands. The pre-edge feature observed in the spectra is directly related to the unoccupied Cu $3d$ band. The angular dependence of the pre-edge peak shows that the Cu $3d$ hole is completely polarized along the *c* axis. The crystal axes direction seems to be more important for the angular dependence than the local axes defined by the distorted oxygen octahedra. The main character of the Cu $3d$ hole obtained from an orbital population analysis is $3d_{xz}$. The dispersion of the Cu $3d$ band expected from previous calculations and confirmed by the experimental data is very small, about 0.6–0.7 eV. The small dispersion and orbital polarization help to explain the relatively weak and anisotropic exchange interactions in $CuGeO_3$. [S0163-1829(99)09719-2]

I. INTRODUCTION

There are several quasi-one-dimensional antiferromagnetic systems that present very interesting physical phenomena. Among them, $CuGeO_3$ was the first inorganic compound known to present the so-called spin-Peierls transition. This is a transition from an antiferromagnetic linear chain to a dimerized (or alternating) singlet chain compound. Because of the spin-Peierls transition, and partly by being a member of the cuprate family, $CuGeO_3$ has attracted considerable attention.

The crystal structure of $CuGeO_3$ is orthorhombic and the lattice parameters are $a=4.81$ Å, $b=8.47$ Å, and $c=2.94$ Å.[1] This quasi-one-dimensional compound presents CuO_6 distorted octahedra sharing edges along the *c* axis; the Cu-O(2) distance to the basal oxygens, 1.94 Å, is shorter than the Cu-O(1) distance to the apical oxygens, 2.76 Å. Hase, Terasaki, and Uchinokura found that the magnetic susceptibility of $CuGeO_3$ dropped abruptly in all directions below 14 K.[2] The expected energy gap in the magnetic excitation spectrum of $CuGeO_3$ was established by inelastic neutron scattering.[3] The singlet-to-triplet character of the magnetic excitations was confirmed by inelastic neutron scattering in a magnetic field.[4] The dimerization of $CuGeO_3$ in the spin-Peierls state was observed by electron, x-ray, and neutron diffraction.[5–7]

There are relatively few experimental studies of the electronic structure of $CuGeO_3$ using direct spectroscopic techniques. Optical reflectivity and x-ray photoelectron spectroscopy confirmed that $CuGeO_3$ is a charge-transfer insulator.[8] Additional optical absorption measurements established that the value of the charge-transfer gap was around 4 eV.[9] Resonant photoemission spectra of $CuGeO_3$ were used to estimate the charge-transfer energy Δ and the Coulomb interaction U.[10] Early band-structure calculations based on the local-density approximation (LDA) predicted a metallic state for $CuGeO_3$.[11,12] Later attempts, which took into account the Coulomb interaction between the $3d$ electrons, gave a band gap of about 3 eV.[13,14]

Unfortunately, there is no information on the unoccupied electronic states or on the angular dependence of these states. Among the open questions, one can mention the character of the first addition state as well as its polarization along the different crystal axes. The purpose of this work is to study the electronic structure of $CuGeO_3$ using angular-resolved Cu *K* -edge x-ray absorption spectroscopy (XAS). The XAS technique is very well suited to address the questions above because it gives site and symmetry selected information.[15] The analysis of the results provides additional information on orbital population, band dispersion, and exchange interactions in this compound.

II. EXPERIMENTAL DETAILS

The $CuGeO_3$ sample was a single crystal grown using the floating zone method; the sample was turquoise, translucent, and highly insulating. The sample had a cylindrical shape with an elliptical cross section; the dimension of the single crystal was approximately $6\times7\times9$ mm ($a\times b\times c$). The sample was cleaved parallel to the bc plane using a sharp blade; the thickness of the resulting slice was less than 100 μm. The magnetic susceptibility of the sample dropped abruptly below 14 K; this signature of the spin-Peierls transition confirmed the quality of the sample.

The x-ray absorption spectra were taken using the DCM beam line at CAMD; this beam line is equipped with a Si(220) double-crystal monochromator.[16] The energy resolution at the Cu *K* absorption edge was approximately 2.3 eV; this value was limited by the angular divergence of the photon beam. The energy scale was calibrated using the known edge position of pure Cu. The spectra were taken in the transmission mode using two ionization chambers; as the thickness of the sample was not changed this method preserved the relative normalization. The edge jump of the spectra, around 2.5, was close to the value that maximizes the signal-to-noise ratio.[17]

The absorption spectra were taken using the linearly polarized light obtained from the orbit plane of the CAMD storage ring. The photon beam was directed along the a axis and the polarization vector of the light was lying in the bc plane. The angle θ between the polarization vector and the c axis was selected rotating the sample around the a axis. It is not possible to study the polarization of the electronic states along the a axis using the present experimental setup; this is not a severe limitation because these states are not expected to play a significant role in this compound.

III. CALCULATION DETAILS

The cluster considered in this calculation consists of a copper ion surrounded by a distorted oxygen octahedra. The germanium levels were not considered in the calculation because they appear at higher energies. The cluster model is solved by the configuration interaction method which takes into account many-body effects.[18,19] The basis functions are ionic configurations that include the possibility of charge transfer from the ligands. The ground state $|\Psi_{GS}\rangle$ can be written as

$$|\Psi_{GS}\rangle=\alpha|3d^9\rangle+\beta|3d^{10}\underline{L}\rangle, \qquad (1)$$

where $3d^n$ corresponds to the metal configuration and $\underline{L}$ denotes a ligand hole.

The main parameters of the calculation are the charge transfer energy Δ, the Coulomb interaction U, and the hybridization T.[18] The splitting of the $3d$ levels and the anisotropy of the hybridization caused by the distortion of the octahedra will be discussed below. The cluster model parameters for $CuGeO_3$ taken from Parmigiani *et al.*[10] are compared to those for CuO in Table I. The most relevant difference is the larger value of Δ, which gives rise to a more ionic ground state and to a larger band gap.[20]

The ground state of $CuGeO_3$ is rather ionic being dominated by the $3d^9$ configuration with an occupancy of around 0.81. The main configuration of the first removal state is $3d^9\underline{L}$ and the first addition state is given by the $3d^{10}$ configuration. This confirms that $CuGeO_3$ is in the charge-transfer regime, as expected for a compound with $U>\Delta$.[21] In this regime, the value of the band gap E_g is closely related, although not exactly equal, to the charge-transfer energy Δ. The value of E_g obtained using the cluster model calculation, 3.5 eV, is in good agreement with the experimental value of 3.7 eV.[10] We note here that the charge transfer regime is a distinct characteristic of the late transition-metal oxides.[22]

TABLE I. Values of the cluster model parameters for CuO and $CuGeO_3$, all values in eV.

Compound	Δ	U	T
CuO	1.8	6.5	−2.0
$CuGeO_3$	4.0	6.5	−2.5

IV. RESULTS AND DISCUSSION

A. Cu *K* absorption edge

Figure 1 compares the Cu *K* x-ray absorption spectra of $CuGeO_3$ taken with $\mathbf{E}\|c$ axis and $\mathbf{E}\|b$ axis to CuO and Cu. These spectra, which correspond to materials with widely different Cu densities, were normalized to the maximum intensity for an easier comparison. The spectra of the reference materials, CuO and Cu, are in excellent agreement with the reported spectra found in the literature. The position of the first inflection point in the spectrum of Cu, around 8979 eV,

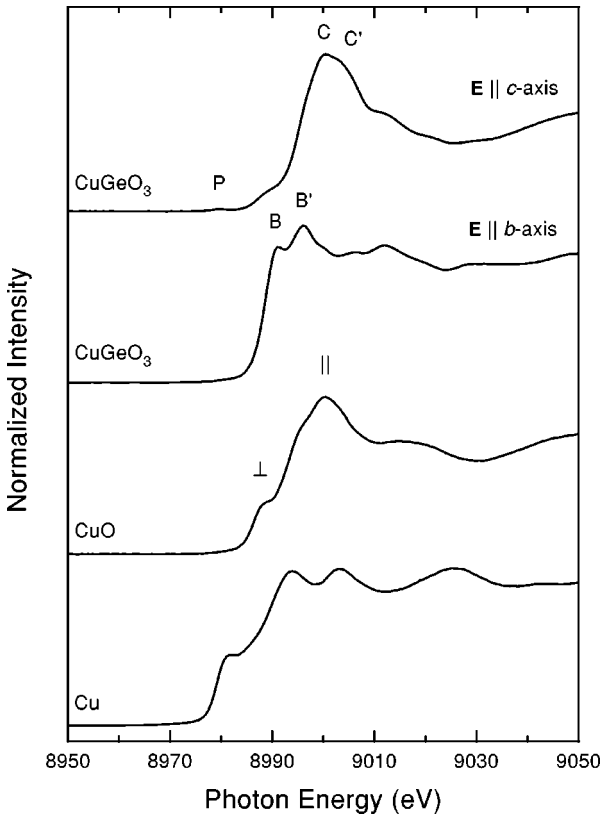

FIG. 1. Cu *K* x-ray absorption spectra of $CuGeO_3$ taken with $\mathbf{E}\|c$ axis and $\mathbf{E}\|b$ axis compared to CuO and Cu.

was used as a reference to calibrate the energy scale. The main contribution to the spectra corresponds to transitions from the Cu $1s$ level to unoccupied Cu $4p$ character in the conduction band. The unoccupied Cu $4p$ character in the spectra of CuO and $CuGeO_3$ is pushed to higher energies because of the antibonding interactions with the O $2p$ levels. The structures observed in the spectra at higher energies, above 9010 eV, are attributed to transitions to unoccupied Cu np character (with $n>4$).

The spectrum of $CuGeO_3$ taken with $\mathbf{E}\|c$ axis corresponds to transitions to unoccupied Cu $4p_z$ character and probes Cu^{2+} ions in a square planar coordination. This spectrum resembles rather closely the spectrum of La_2CuO_4 taken with $\mathbf{E}\|ab$ plane, which also probes Cu^{2+} ions in a square plane coordination.[23] Following this work on La_2CuO_4, we attribute the main peak in the $\mathbf{E}\|c$ axis spectrum of $CuGeO_3$ (C) to the antibonding Cu $4p_z$ band. On the other hand, the spectrum of $CuGeO_3$ taken with $\mathbf{E}\|b$ axis corresponds to transitions to unoccupied Cu $4p_y$ character probing Cu^{2+} ions in a linear coordination. This spectrum is rather similar to the spectrum of La_2CuO_4 taken with $\mathbf{E}\perp ab$ plane, which also probes Cu^{2+} ions in a linear coordination.[23] Following this work on La_2CuO_4, we attribute the first peak in the $\mathbf{E}\|b$ axis spectrum of $CuGeO_3$ (B) to the antibonding Cu $4p_y$ band. The spectrum of CuO probes Cu^{2+} ions in a distorted square planar coordination; since the sample is polycrystalline, $\mathbf{E}$ may probe states parallel or perpendicular to the coordination plane. The main peak in the spectrum ($\|$) is attributed to Cu $4p$ states polarized parallel to the coordination plane, whereas the shoulder at smaller energies ($\perp$) is ascribed to Cu $4p$ states polarized perpendicular to the coordination plane.

We note that the Cu $4p_z$ band in the $\mathbf{E}\|c$ axis spectrum is located at higher energies than the Cu $4p_y$ band in the $\mathbf{E}\|b$ axis spectrum. The Cu $4p_z$ band is pushed higher in energy than the Cu $4p_y$ band because the Cu $4p_z$-O $2p$ antibonding interactions are stronger than the Cu $4p_y$-O $2p$ interactions. These interactions are proportional to the Slater-Koster parameter $(pp\sigma)$ which is known to scale as $1/R^2$; where R denotes the interatomic Cu-O distance.[24] The shorter Cu-O(2) distance to the basal oxygens, 1.94 Å, gives rise to a larger $(pp\sigma)$ parameter and to stronger Cu $4p_z$-O $2p$ antibonding interactions, whereas the larger Cu-O(1) distance to the apical oxygens, 2.76 Å, results in a smaller $(pp\sigma)$ parameter and to weaker Cu $4p_y$-O $2p$ interactions. A similar argument was invoked to explain the energy difference between the Cu $4p_{x,y}$ and Cu $4p_z$ bands in the Cu K x-ray absorption spectra of La_2CuO_4.[23]

The peaks associated with the Cu $4p_z$ and $4p_y$ bands in the spectra of $CuGeO_3$ (C and B) are followed by peaks at approximately 5 eV higher energies (C' and B'). The main peaks correspond to the so-called *well screened* final states, whereas the satellite peaks are attributed to the *poorly screened* final states. The *well screened* peak corresponds to a final state that is dominated by the $|\underline{c}3d^{10}\underline{L}4p\rangle$ configuration, whereas the main component of the *poorly screened* peak is given by the $|\underline{c}3d^9 4p\rangle$ configuration, where $\underline{c}$ denotes a hole in the Cu $1s$ level. The *poorly screened* satellite is particularly strong in this case because the excited electron, Cu $4p$, is not the natural screening electron, Cu $3d$. We note here that in the Cu $L_{2,3}$ absorption edge, where the excited electron acts as the screening electron, the *poorly screened* satellite is barely observed.[25] The energy difference ΔE between the *well screened* and *poorly screened* peaks, within the cluster model approximation, is given by $\Delta E^2 = (Q-\Delta)^2 + 4T^2$; where Q denotes the Coulomb interaction between the Cu $1s$ core hole and the screening electron in the Cu $3d$ orbital. Taking $Q \simeq 7$ eV, $\Delta \simeq 4$ eV, and $T \simeq 2.5$ eV, we obtain $\Delta E \simeq 5$ eV which is in very good agreement with the experimental splitting.

The spectrum of $CuGeO_3$ taken with $\mathbf{E}\|c$ axis presents a weak pre-edge feature (P) below the absorption edge, around 8979 eV. This pre-edge feature corresponds to electric dipole forbidden transitions from the Cu $1s$ level to unoccupied Cu $3d$ character. The main channels for this transition are (a) *indirect electric dipole* transitions to Cu $4p$ character mixed with Cu $3d$ states at neighboring sites, and (b) *direct electric quadrupole* transitions from the Cu $1s$ level to Cu $3d$ character at the absorbing site. This assignment is in agreement with the analysis of the pre-edge features observed in the Ti K x-ray absorption spectra of titanium oxide.[26,27] We note here that *direct magnetic dipole* transitions from the Cu $1s$ level to Cu $3d$ character at the absorbing site are much weaker and can be neglected.[28] In this case, the *poorly screened* satellite associated with the pre-edge peak is not observed because the transition reaches the natural screening electron. Despite its weakness, the information provided by the pre-edge feature is very important because it probes directly the Cu $3d$ hole, as discussed below.

B. Angular dependence

Figure 2 shows the Cu K x-ray absorption spectra of $CuGeO_3$ taken at different angles θ between the polarization vector of the light and the c axis. The polarization vector was lying in the bc plane, so $\theta = 0°$ corresponds to the $\mathbf{E}\|c$ axis spectrum and $\theta = 90°$ to the $\mathbf{E}\|b$ axis spectrum. The edge jump of each spectrum was divided by the same constant factor thus preserving the relative intensity normalization. The spectra show dramatic changes in the region attributed to the Cu $4p_z$ (C and C') and the Cu $4p_y$ (B and B') bands, and much weaker changes in the region ascribed to the Cu np bands above 9010 eV. As expected, the intensities of the Cu $4p_z$ band peaks are larger for small angles where $\mathbf{E}\|c$ axis, whereas the intensities of the Cu $4p_y$ band peaks are larger for large angles where $\mathbf{E}\|b$ axis.

In principle, the intensity of the Cu $4p_z$ band features should exhibit a $\cos^2\theta$ angular dependence, whereas the intensity of the Cu $4p_y$ band features should behave as $\sin^2\theta$. A more detailed analysis of the angular variation in the spectra is hampered by the overlap, mixing, and the dispersion of the different subbands. In particular, we note that (a) the B' peak corresponding to the Cu $4p_y$ band partially overlaps the C peak corresponding to the Cu $4p_z$ band, (b) there is considerable band mixing because the crystal axes do not coincide with the local coordination axes,[29] and (c) the dispersion of the bands generates energy shifts in the position of the peaks as the angle is changed.

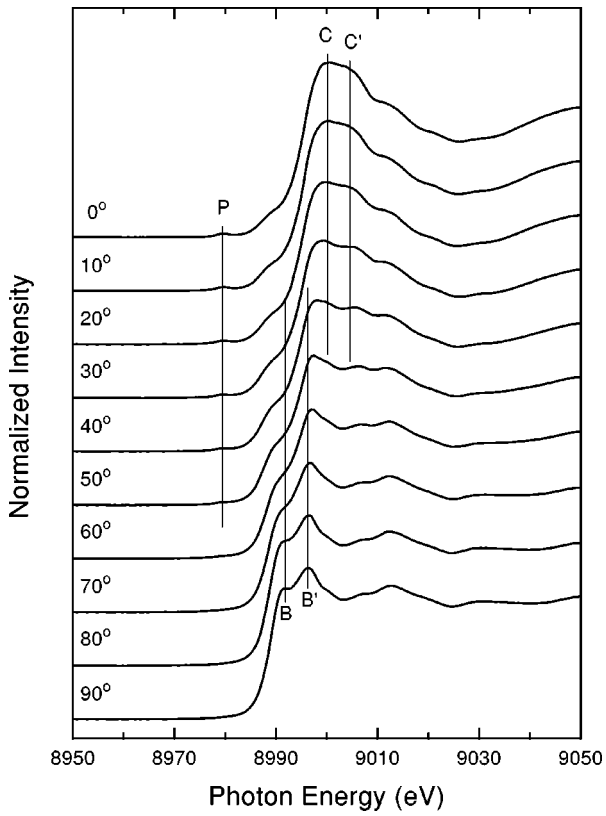

FIG. 2. Cu *K* x-ray absorption spectra of $CuGeO_3$ taken as a function of the angle θ between the polarization vector of the light and the *c* axis.

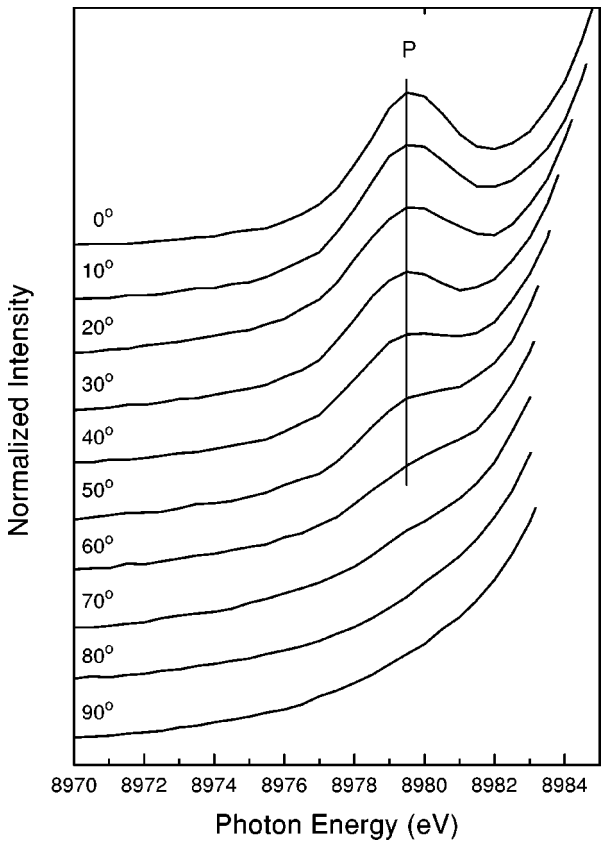

FIG. 3. Pre-edge feature in the Cu *K* absorption edge of $CuGeO_3$ as a function of the angle θ between the polarization vector and the *c* axis.

The dispersion can be clearly observed in the *B* peak corresponding to the Cu $4p_y$ band which shifts to lower energies as the angle is decreased. This effect can be also observed in the C' peak corresponding to the Cu $4p_z$ band which shifts to higher energies as the angle is increased. In principle, all the different Cu $4p$ subbands observed in the spectra are expected to present a certain degree of dispersion. Again, the dispersion of a given subband can not always be isolated because of the overlap and the mixing between the different bands.

The best way to analyze the overlap, mixing, and dispersion of the unoccupied Cu $4p$ bands would be with the aid of band-structure calculations. Unfortunately, calculations of the higher energy unoccupied electronic states in $CuGeO_3$ are not readily available in the literature. The splitting of the spectral weight into *well screened* and *poorly screened* peaks further complicates a quantitative analysis of the spectra. This many-body effect, caused by the switching on of the Cu $1s$ core-hole potential in the final state, is difficult to include in the calculations. Another alternative method to analyze the spectra would be the use of the well-known multiple-scattering formalism;[30,31] unfortunately the use of this single-particle approach for highly correlated systems like $CuGeO_3$ is not fully justified.

The intensity of the pre-edge feature (*P*) probing the Cu $3d$ hole is larger for small angles, where $\mathbf{E}\|c$ axis, and diminishes for larger angles. The energy position of the pre-edge peak does not change as the angle is increased indicating that the dispersion of the Cu $3d$ band is very small. The angular dependence of the pre-edge peak intensity indicates that the Cu $3d$ hole in $CuGeO_3$ is mostly polarized along the *c* axis. This behavior was expected taking into account the quasi-one-dimensional character and the observed physical properties of this compound. This pre-edge feature is particularly important because it is directly related to the Cu $3d$ band and deserves to be analyzed in more detail.

C. Pre-peak feature

Figure 3 shows the pre-edge feature in the Cu *K* absorption edge of $CuGeO_3$ as a function of the angle θ between the polarization vector and the *c* axis. The polarization vector was lying in the *bc* plane, so $\theta=0°$ corresponds to the $\mathbf{E}\|c$ axis spectrum and $\theta=90°$ to the $\mathbf{E}\|b$ axis spectrum. The edge jump of each spectrum was divided by the same constant factor so as to preserve the relative intensity normalization. The pre-edge peak (*P*) probing the Cu $3d$ hole is mounted on a rising background which corresponds to the tail of the Cu $4p$ band features appearing at higher energies. The intensity of the pre-edge peak is larger for small angles, where $\mathbf{E}\|c$ axis, dercreases for larger angles, and disappears completely for $\theta=90°$. These results show convincingly that the unoccupied Cu $3d$ state in this compound is completely polarized along the *c* axis.

The pre-edge feature in the spectra corresponds to electric dipole forbidden transitions from the Cu $1s$ level to unoccupied Cu $3d$ states. The main channels are (a) *indirect electric dipole* transitions to Cu $4p$ character mixed with Cu $3d$ states at neighboring sites, and (b) *direct electric*

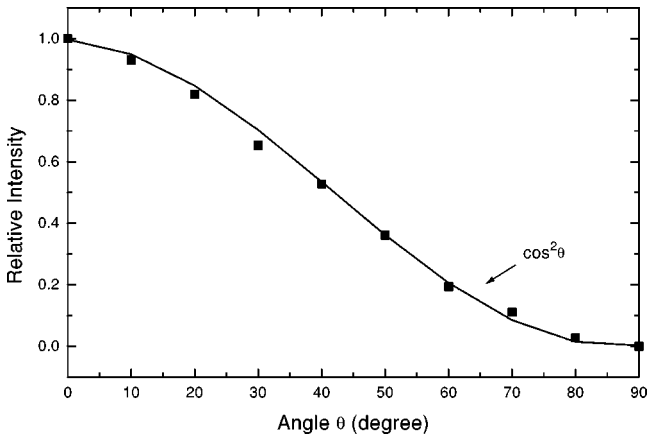

FIG. 4. Intensity of the pre-edge feature in the Cu *K* absorption edge of $CuGeO_3$ as a function of the angle θ between the polarization vector and the *c* axis.

quadrupole transitions to Cu $3d$ character at the absorbing site. In the present setup, the expected angular dependence of the transitions to the polarized Cu $3d$ hole should be $\cos^2\theta$ for both channels. In addition, the expected splitting of these transitions is less evident than in the pre-edge features observed in the Ti *K*-edge spectra of TiO_2.[26,27] For these reasons, it is very difficult to isolate the contribution of the *indirect electric dipole* and *direct electric quadrupole* channels.

We note that the general angular dependence of the pre-edge peak involves a series of products of trigonometric functions that depend on the angles between the photon direction, the polarization vector, and the crystal axes. The intensity of the pre-edge peak may display a very complex behavior with angle and even a $\cos^4\theta$ angular dependence can be experimentally realized.[28] The relatively simple $\cos^2\theta$ angular dependence obtained in this case is due to our particular choice of the experimental geometry.

Figure 4 shows the intensity of the pre-edge feature as a function of the angle θ between the polarization vector of the light and the *c* axis. The intensity of the feature was obtained by fitting the pre-edge peak with a Lorentzian function and the background with a Lorentzian tail. The fitting procedure with these functions gave very good results, a particular example of the fitting result for $\theta=0°$ is presented below. The experimental points obtained from the fitting follow rather closely the expected $\cos^2\theta$ angular dependence illustrated by the solid line.[32]

The pre-edge feature can be well explained by a single Lorentzian function whose width and position do not change with the angle. This result indicates that the unoccupied Cu $3d$ band probed by the pre-edge feature exhibits a very small band dispersion. In turn, the small Cu $3d$ band dispersion helps to explain the relatively weak exchange interactions observed in this compound, as discussed below. Figure 5(a) illustrates the fitting of the pre-peak feature for $\theta=0°$: experiment (points), fitting (solid line), pre-edge peak (dotted line), and background (dashed line). The functional dependence chosen for the fit gives a very good agreement between the fitting result and the experimental points.

Figures 5(b) and 5(c) compare the pre-edge feature for $\theta=0°$ to LDA + U[13] and Hartree-Fock[14] band-structure calculations. The energy scale of the theoretical calculations was shifted by hand so as to get the best possible match with the pre-edge feature. The full width at half maximum of the pre-edge feature, 2.9 eV, is much larger than the calculated dispersion of the unoccupied Cu $3d$ band, 0.6 eV.[13,14] The main contribution to the broadening of the pre-edge peak comes from the experimental resolution, 2.3 eV, and the Cu $1s$ lifetime broadening, 1.6 eV.[15] We note that the width of the Cu $3d$ band estimated from the O *K* x-ray absorption edge, 0.7 eV, is in good agreement with the calculated dispersion, 0.6 eV;[33] this estimation is more reliable because the O *K* x-ray absorption edge is much less affected by the experimental resolution and the O $1s$ lifetime broadening. According to the LDA + U calculation,[13] the unoccupied Cu $3d$ band probed by the pre-edge feature is formed by Cu $3d_{xz}$ states. This assignment is in good agreement with the result of the orbital population analysis based on the cluster model calculation discussed below.

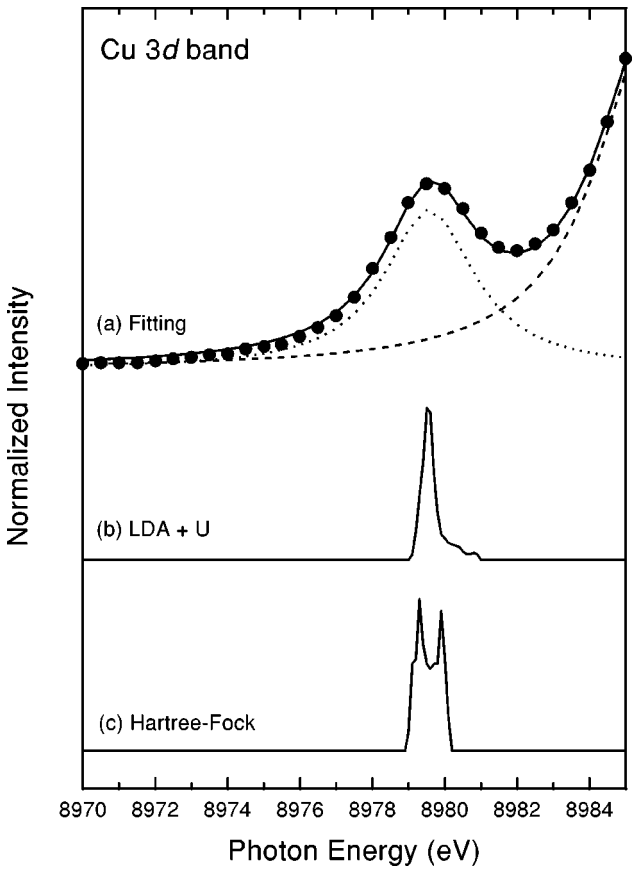

FIG. 5. Comparison betweem the pre-edge feature in the Cu *K* absorption edge of $CuGeO_3$ ($\theta=0$) and band-structure calculations: (a) fitting, (b) LDA + U, and (c) Hartree-Fock.

D. Orbital population

Figure 6(a) shows the splitting of the Cu $3d$ levels induced by crystal-field effects in octahedral (O_h) and tetragonal (D_{4h}) symmetry.[34] The ordering of the energy levels follows the relative strength of the Cu $3d$-O $2p$ interactions; the levels with the higher energies correspond to the stronger interactions. The highest energy level corresponds to the $3d_{xz}$ state that points directly to the basal oxygens

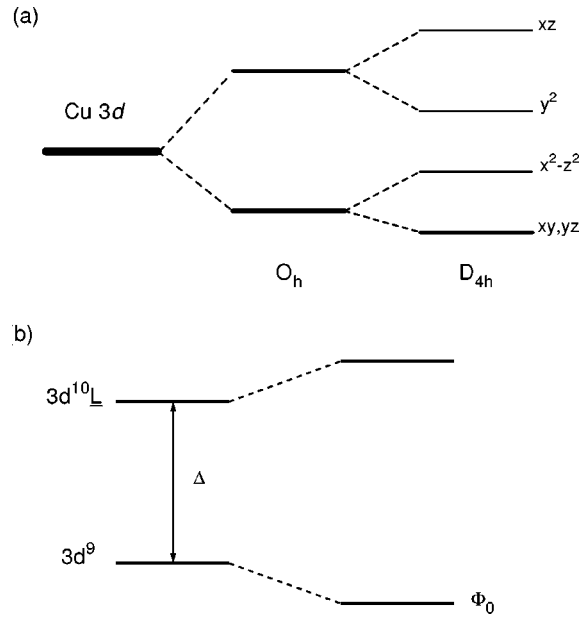

FIG. 6. (a) Splitting of the Cu $3d$ energy levels by crystal-field effects in octahedral and tetragonal symmetry. (b) Hybridization of the electronic configurations used in the calculation of the ground state of $CuGeO_3$.

located at a relatively shorter distance. According to this energy-level diagram, the main character of the Cu $3d$ hole in the $CuGeO_3$ compound should be $3d_{xz}$. Unfortunately, the crystal-field approach is not entirely reliable because it does not take into account the Cu $3d$-O $2p$ hybridization.

Figure 6(b) illustrates the stabilization of the ground state due to the mixture of configurations in the cluster model approximation. The largest stabilization is obtained for a configuration with a Cu $3d_{xz}$ hole, because this state produces the largest hybridization with the O $2p$ orbitals. Therefore, both the crystal-field and the cluster model approaches indicate that the unoccupied portion of the Cu $3d$ band is formed by Cu $3d_{xz}$ states. This conclusion is in agreement with the LDA + U band-structure calculation[13] and is consistent with the quasi-one-dimensional character of this compound.

The results show that the Cu $3d$ unoccupied electronic states probed by the pre-edge feature are completely polarized along the *c* axis. The crystal axes direction seems to be more important for the angular dependence than the local axes defined by the distorted oxygen octahedra. The same behavior was observed in the N $1s$ x-ray absorption spectra of the quasi-one-dimensional $(DMe\text{-}DCNQI\text{-}d_7)_2Cu$ organic compound.[35] It is often assumed that the electronic structure of highly correlated systems is completely dominated by short-range order and localized interactions. These examples show that long-range order and band-structure effects also play an important role in the electronic structure of these materials.[36]

The interatomic exchange interaction J_c of $CuGeO_3$ along the *c* axis, about 10 meV, is relatively small compared to that found in the corner sharing antiferromagnetic cuprates, around 100 meV. This interaction is mediated by indirect Cu $3d$-O $2p$-Cu $3d$ charge fluctuations that, in turn, are also responsible for the dispersion of the Cu $3d$ band. Therefore, the small dispersion of the Cu $3d$ band deduced from the experimental data helps to explain the relatively small exchange interaction in $CuGeO_3$. We also note that the interatomic exchange interaction of $CuGeO_3$ along the *c* axis, $J_c \approx 10$ meV, is much larger than along the *b* axis, $J_b \approx 1$ meV.[3] This is attributed not only to smaller Cu $3d$-O $2p$-Cu $3d$ interactions along the *b* axis, but also to the Cu $3d_{xz}$ orbital polarization that leave no phase space available for charge fluctuations along this direction.

V. SUMMARY AND CONCLUSIONS

In summary, we studied the unoccupied electronic states of $CuGeO_3$ using linearly polarized Cu *K*-edge absorption spectroscopy. The spectra show structures related to the Cu $4p_z$ band with $\mathbf{E}\|c$ axis and to the Cu $4p_y$ band with $\mathbf{E}\|b$ axis. The Cu $4p_z$ band appears at higher energies than the Cu $4p_y$ band due to the stronger interactions with the O $2p$ levels. The Cu $4p$ spectral weight is split about 5 eV into the so-called *well screened* and *poorly screened* peaks. The Cu $4p$ bands exhibit changes as a function of the angle θ between the polarization vector and the *c* axis. The intensity changes reflect the polarization and the energy shifts reflect the dispersion of the Cu $4p$ bands.

The pre-edge feature observed in the spectra is directly related to the unoccupied Cu $3d$ band. The angular dependence of the pre-edge peak shows that the Cu $3d$ hole is completely polarized along the *c* axis. The crystal axes direction seems to be more important for the angular dependence than the local axes defined by the distorted oxygen octahedra. The main character of the Cu $3d$ hole obtained from an orbital population analysis is $3d_{xz}$. The dispersion of the Cu $3d$ band expected from previous calculations and confirmed by the experimental data is very small, about 0.6–0.7 eV. The small dispersion and the orbital polarization help to explain the relatively weak and anisotropic exchange interactions in $CuGeO_3$.

ACKNOWLEDGMENTS

This work was partially supported by Fundação de Amparo a Pesquisa do Estado de São Paulo (Processo No. 96/12084-7), Conselho Nacional de Desenvolvimento Científico e Tecnológico (Processo No. 300483/96-1), National Science Foundation (Contract No. INT-9512916), New Energy and Industrial Development Organization (NEDO), and a Grant-in-Aid for Scientific Research of the Ministry of Education, Science, Culture and Sports of Japan.

*Author to whom correspondence should be addressed.
FAX: + (55) (41) 361-3418.
Electronic address: miguel@fisica.ufpr.br

[1] H. Völlenkle, A. Wittmann, and H. Nowotny, Monatsch. Chem. **98**, 1352 (1957).
[2] M. Hase, I. Terasaki, and K. Uchinokura, Phys. Rev. Lett. **70**, 3651 (1993).
[3] M. Nishi, O. Fujita, and J. Akimitsu, Phys. Rev. B **50**, 6508

(1994).
[4] O. Fujita, J. Akimitsu, M. Nishi, and K. Kakurai, Phys. Rev. Lett. **74**, 1677 (1995).
[5] O. Kamimura, M. Terauchi, M. Tanaka, O. Fujita, and J. Akimitsu, J. Phys. Soc. Jpn. **63**, 2467 (1994).
[6] J.P. Pouget, L.P. Regnault, M. Ain, B. Hennion, J.P. Renard, P. Veillet, G. Dhalenne, and A. Revcolevschi, Phys. Rev. Lett. **72**, 4037 (1994).
[7] K. Hirota, D.E. Cox, J.E. Lorenzo, G. Shirane, J.M. Tranquada, M. Hase, K. Uchinokura, H. Kojima, Y. Shibuya, and I. Tanaka, Phys. Rev. Lett. **73**, 736 (1994).
[8] I. Terasaki, R. Itti, N. Koshizuka, M. Hase, I. Tsukada, and K. Uchinokura, Phys. Rev. B **52**, 295 (1995).
[9] M. Bassi, P. Camagni, R. Rolli, G. Samoggia, F. Parmigiani, G. Dhalenne, and A. Revcolevschi, Phys. Rev. B **54**, R11 030 (1996).
[10] F. Parmigiani, L. Sangaletti, A. Goldoni, U. del Pennino, C. Kim, Z.X. Shen, A. Revcolevschi, and G. Dhalenne, Phys. Rev. B **55**, 1459 (1997).
[11] L.F. Mattheiss, Phys. Rev. B **49**, 14 050 (1994).
[12] Z.S. Popovic, F.R. Vukajlovic, and Z.V. Sljivancanin, J. Phys.: Condens. Matter **7**, 4549 (1995).
[13] Z.V. Sljivancanin, Z.S. Popovic, and F.R. Vukajlovic, Phys. Rev. B **56**, 4432 (1997).
[14] S. Zagoulaev and I.I. Tupitsyn, Phys. Rev. B **55**, 13 528 (1997).
[15] *Unoccupied Electronic States*, edited by J.C. Fuggle and J.E. Inglesfield (Springer, Berlin, 1992).
[16] P.J. Schilling, E. Morikawa, H. Tolentino, E. Tamura, R.L. Kurtz, and C. Cusatis, Rev. Sci. Instrum. **66**, 2214 (1995).
[17] S. M. Heald, in *X-Ray Absorption Spectroscopy: Principles, Applications, Techniques of EXAFS, SEXAFS and XANES*, edited by D. C. Koningsberg and R. Prins (Wiley, New York, 1988).
[18] G. van der Laan, C. Westra, C. Haas, and G.A. Sawatzky, Phys. Rev. B **23**, 4369 (1981).
[19] A. Fujimori and F. Minami, Phys. Rev. B **30**, 957 (1984).
[20] H. Eskes, L.H. Tjeng, and G.A. Sawatzky, Phys. Rev. B **41**, 288 (1990).
[21] J. Zaanen, G.A. Sawatzky, and J.W. Allen, Phys. Rev. Lett. **55**, 418 (1985).
[22] M. Abbate, F.M.F. de Groot, J.C. Fuggle, A. Fujimori, Y. Tokura, Y. Fujishima, O. Strebel, M. Domke, G. Kaindl, J. van Elp, B.T. Thole, G.A. Sawatzky, M. Sacchi, and N. Tsuda, Phys. Rev. B **44**, 5419 (1991).
[23] H. Tolentino, M. Medarde, A. Fontaine, F. Baudelet, E. Dartyge, D. Guay, and G. Tourillon, Phys. Rev. B **45**, 8091 (1992); H. Tolentino, M. Medarde, A. Fontaine, F. Baudelet, and E. Dartyge, J. Electron Spectrosc. Relat. Phenom. **62**, 167 (1993).
[24] W. A. Harrison, *Electronic Structure and the Properties of Solids* (Freeman, New York, 1980).
[25] M. Abbate, M. Sacchi, J.J. Wnuk, L.W.M. Schreurs, Y.S. Wang, R. Lof, and J.C. Fuggle, Phys. Rev. B **42**, 7914 (1990).
[26] T. Uozumi, K. Okada, A. Kotani, O. Durmeyer, J.P. Kappler, E. Beaurepaire, and J.C. Parlebas, Europhys. Lett. **18**, 85 (1992).
[27] E. Beaurepaire, S. Lewonczuk, J. Ringeissen, J.C. Parlebas, T. Uozumi, K. Okada, and A. Kotani, Europhys. Lett. **22**, 463 (1993).
[28] C. Brouder, J. Phys.: Condens. Matter **2**, 701 (1990).
[29] The difference between the crystal axes and the local axes is illustrated, for instance, in Fig. 1 of Ref. 11.
[30] Z.Y. Wu, S. Gota, F. Jollet, M. Pollak, M. Gautier-Soyer, and C.R. Natoli, Phys. Rev. B **55**, 2570 (1997).
[31] A.L. Ankudinov, B. Ravel, J.J. Rehr, and S.D. Conradson, Phys. Rev. B **58**, 7565 (1998).
[32] The $\cos^2\theta$ angular dependence was shifted by $-3°$ to take into account a slight angular misalignment in the experimental setup.
[33] D.Z. Cruz *et al.* (unpublished).
[34] S. Sugano, Y. Tanabe, and H. Kamimura, *Multiplets of Transition-Metal Ions in Crystals* (Academic, New York, 1970).
[35] A. Sekiyama, A. Fujimori, S. Aonuma, and R. Kato, Phys. Rev. B **56**, 9937 (1997).
[36] *Narrow Band Phenomena*, edited by J.C. Fuggle, G.A. Sawatzky, and J.W. Allen (Plenum, New York, 1988).